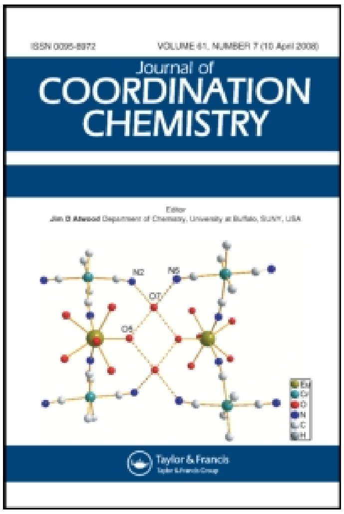

Journal of Coordination Chemistry
Publication details, including instructions for authors and subscription information:
http://www.informaworld.com/smpp/title~content=t713455674

Hydrothermal syntheses and crystal structures of two organic-inorganic hybrid molybdovanadates based on $[V_2Mo_6(OH)_2O_{24}]^{4-}$ and $[VMo_{12}O_{40}]^{3-}$ polyoxoanions

Jingping Wang[a]; Yuquan Feng[a]; Junwei Zhao[a]; Pengtao Ma[a]; Xinfang Zhang[a]; Jingyang Niu[a]
[a] Institute of Molecular and Crystal Engineering, School of Chemistry and Chemical Engineering, Henan University, Kaifeng 475004, P.R. China

To cite this Article Wang, Jingping , Feng, Yuquan , Zhao, Junwei , Ma, Pengtao , Zhang, Xinfang and Niu, Jingyang(2009) 'Hydrothermal syntheses and crystal structures of two organic-inorganic hybrid molybdovanadates based on $[V_2Mo_6(OH)_2O_{24}]^{4-}$ and $[VMo_{12}O_{40}]^{3-}$ polyoxoanions', Journal of Coordination Chemistry, 62: 23, 3754 — 3762
To link to this Article: DOI: 10.1080/00958970903161301
URL: http://dx.doi.org/10.1080/00958970903161301

Journal of Coordination Chemistry
Vol. 62, No. 23, 10 December 2009, 3754–3762

Hydrothermal syntheses and crystal structures of two organic–inorganic hybrid molybdovanadates based on $[V_2Mo_6(OH)_2O_{24}]^{4-}$ and $[VMo_{12}O_{40}]^{3-}$ polyoxoanions

JINGPING WANG, YUQUAN FENG, JUNWEI ZHAO, PENGTAO MA,
XINFANG ZHANG and JINGYANG NIU*

Institute of Molecular and Crystal Engineering, School of Chemistry and Chemical Engineering, Henan University, Kaifeng 475004, P.R. China

(*Received 18 February 2009; in final form 16 May 2009*)

Two new organic–inorganic hybrid cobalt-molybdovanadates $[Co(phen)_3]H_2[H_2V_2Mo_6O_{26}] \cdot 7H_2O$ (**1**) and $[Co(2,2'\text{-bipy})_3][Na(H_2O)_7][VMo_{12}O_{40}]$ (**2**) have been hydrothermally synthesized and structurally characterized by elemental analyses, IR, UV, XPS spectroscopy, thermogravimetric (TG) analyses, and X-ray single crystal diffraction. The molecular structure of **1** consists of a $[V_2Mo_6(OH)_2O_{24}]^{4-}$ polyoxoanion, a $[Co(phen)_3]^{2+}$, two H^+ and seven lattice water molecules. The structure of $[V_2Mo_6(OH)_2O_{24}]^{4-}$ consists of six MoO_6 octahedra and two VO_4 tetrahedra; six MoO_6 octahedra are linked by edge-sharing oxygens forming a $\{Mo_6\}$ ring, and two VO_4 tetrahedra cap opposite sides of the $\{Mo_6\}$ ring. The molecular structural unit of **2** is constructed from a typical Keggin-type $[VMo_{12}O_{40}]^{3-}$ polyoxoanion and a $[Co(2,2'\text{-bipy})_3]^{2+}$ cation and a Na^+ countercation; Co^{2+} is coordinated by six nitrogens from three 2,2′-bipyridines forming a distorted octahedron.

Keywords: Cobalt-molybdovanadate; Hydrothermal synthesis; Crystal structure; XPS spectra

1. Introduction

Design and synthesis of molecule-based materials with electrical, magnetic, and optic properties have become a focus of interest [1, 2]. Many studies have shown that these properties are intimately related to microstructures in the atomic and molecular levels constructed by the so-called anion–cation salts or host–guest solids [2]. Polyoxometalate (POM) chemistry has drawn interest from both the fundamental and the practical view. POMs are versatile inorganic building blocks for molecule-based materials because of their ability to accept electrons and compositional tunability [3]. An important advance in POM chemistry is designing and assembling organic–inorganic hybrid polyoxomolybdates owing to their pronounced structural diversity and unusual physicochemical properties [4, 5]. Reported polyoxomolybdates were mostly vanadium-containing molybdophosphates [6–8]; however, investigations on $[V_2Mo_6(OH)_2O_{24}]^{4-}$ or $[VMo_{12}O_{40}]^{3-}$ polyoxoanions and their derivatives remain largely unexplored [9, 10].

---

*Corresponding author. Email: jyniu@henu.edu.cn

Journal of Coordination Chemistry
ISSN 0095-8972 print/ISSN 1029-0389 online
DOI: 10.1080/00958970903161301

Especially, these compounds exhibit important catalytic activities for redox reactions [11] and their formation conditions are critical. Therefore, the design and synthesis of these kinds of compounds remains a challenge. We are exploiting the transition-metal/vanadium/molybdenum system in the presence of rigid aromatic nitrogen ligands (phen, 2,2′-bipy, 4,4′-bipy) by hydrothermal synthesis and have isolated two organic–inorganic hybrid cobalt-molybdovanadates $[Co(phen)_3]H_2[V_2Mo_6(OH)_2O_{24}] \cdot 7H_2O$ (**1**) and $[Co(2,2'\text{-bipy})_3]$ $[Na(H_2O)_7][VMo_{12}O_{40}]$ (**2**). In this article, we report the syntheses and structural characterization by elemental analyses, IR, UV, XPS spectroscopy, TG analyses, and X-ray single crystal diffraction.

2. Experimental

2.1. *Materials and physical measurements*

All chemicals were obtained from commercial sources and are used without purification. C, H, and N elemental analyses were performed on a Perkin-Elmer 240C elemental analyzer. IR spectra were recorded on a Nicolet 170FT-IR spectrometer using KBr pellets from 4000 to 400 cm^{-1}. UV spectra were recorded with a U-4100 spectrometer (distilled water as solvent) from 400 to 190 nm. XPS spectra were obtained on an AXIS ULTRA spectrometer with an Al Kα ($hv = 1486.7$ eV) achromatic X-ray source. Thermogravimetric (TG) analyses were performed on a Perkin-Elmer 7 thermal analysis instrument in flowing N_2 with a heating rate of 10°C min^{-1} from 20°C to 700°C.

2.2. *Preparation of $[Co(phen)_3]H_2[V_2Mo_6(OH)_2O_{24}] \cdot 7H_2O$ (1)*

Crystals of **1** were prepared from a reaction mixture of $Co(NO_3)_2 \cdot 6H_2O$ (0.55 mmol, 0.16 g), V_2O_5 (0.55 mmol, 0.10 g), $Na_2MoO_4 \cdot 2H_2O$ (3.2 mmol, 1.49 g), phen (0.25 mmol, 0.05 g), and water (12 mL). The mixture was carefully adjusted to $pH = 5.5$ by addition of 4 mol L^{-1} HCl (aqueous) and then stirred for 0.5 h in air. The final solution was transferred into a Teflon-lined stainless steel autoclave (30 mL) and heated to 180°C for 80 h. After the mixture was slowly cooled to room temperature, yellow block-shaped crystals were filtered off, washed with distilled water, and air-dried. Yield: ca. 60% based on $Co(NO_3)_2 \cdot 6H_2O$. Anal. Calcd for $[Co(phen)_3]H_2[V_2Mo_6(OH)_2O_{24}] \cdot 7H_2O$: C, 23.79; H, 2.27; N, 4.58%. Found: C, 23.72; H, 2.32; N, 4.61%.

2.3. *Preparation of $[Co(2,2'\text{-bipy})_3][Na(H_2O)_7][VMo_{12}O_{40}]$ (2)*

A mixture of $Co(NO_3)_2 \cdot 6H_2O$ (0.30 mmol, 0.09 g), V_2O_5 (0.15 mmol, 0.03 g), $Na_2MoO_4 \cdot 2H_2O$ (3.2 mmol, 1.49 g), 2,2′-bipy (0.32 mmol, 0.05 g), and water (12 mL) was stirred for 2 h in air, then the pH was carefully adjusted to 4.7 with 4 mol L^{-1} HCl. The resulting mixture was transferred to a Teflon-lined stainless steel autoclave (30 mL) and kept at 180°C for 144 h. The yellow block crystals of **2** were filtered off after the autoclave was slowly cooled to room temperature (2 days), washed with distilled water and air-dried at room temperature. Yield: ca 40% based on $Co(NO_3)_2 \cdot 6H_2O$.

Table 1. Crystallographic data and structural refinements for **1** and **2**.

	1	**2**
Empirical formula	$C_{36}H_{42}N_6CoMo_6V_2O_{33}$	$C_{30}H_{38}CoMo_{12}N_6NaO_{47}V$
Formula weight	1823.20	2518.78
Temperature (K)	293(2)	293(2)
Wavelength (Å)	0.71073	0.71073
Crystal system	Monoclinic	Trigonal
Space group	*C2/c*	*R3/c*
Unit cell dimensions (Å, °)		
a	13.4719(14)	12.997(10)
b	17.3696(17)	12.997(10)
c	25.282(2)	62.35(10)
α	90	90
β	92.130(2)	90
γ	90	120
Volume (Å^3), *Z*	5912.0(10), 4	9121(17), 6
Calculated density (Mg m^{-3})	2.028	2.736
Absorption coefficient (mm^{-1})	1.896	2.916
Max. and min. transmission	0.7906 and 0.6695	0.7210 and 0.6688
Refinement method	Full-matrix least-squares on F^2	Full-matrix least-squares on F^2
Data/restraints/parameters	5076/36/439	3594/15/302
Goodness-of-fit on F^2	1.005	1.091
Final *R* indices [$I > 2\sigma(I)$]	0.0553	0.0437
wR (all data)	0.1482	0.0999
Largest difference peak and hole (e Å^{-3})	1.799 and −0.786	1.111 and −1.088

Anal. Calcd for $[Co(2,2'\text{-bipy})_3][Na(H_2O)_7][VMo_{12}O_{40}]$: C, 14.23; H, 1.61; N, 3.37%. Found: C, 14.31; H, 1.52; N, 3.34%.

2.4. *Single crystal X-ray diffraction study of 1 and 2*

Crystal structures of **1** and **2** were determined from single crystal X-ray diffraction data. Intensity data were collected on a Bruker APEX-CCD diffractometer at 296 K using Mo-Kα radiation ($\lambda = 0.71073$ Å). The structures were solved by direct methods and refined by full-matrix least-squares on F^2 using SHELXTL-97. All nonhydrogen atoms were refined anisotropically. The organic hydrogens were generated geometrically. In **2**, Na1 and Na2 ions are disordered with occupancy of 73% and 27%, respectively. The crystal data and structural refinements of **1** and **2** are summarized in table 1. Selected bond lengths (Å) and angles (°) are listed in table 2 for **1** and table 3 for **2**, respectively.

3. Results and discussion

3.1. *Synthesis*

Owing to complicated and largely unknown reaction mechanisms, it is quite difficult to design straightforward synthetic routes to organic–inorganic hybrid POMs by conventional aqueous solution method. Hydrothermal synthesis has proved to be

Table 2. Selected bond distances (Å) and angles (°) for **1**.

Co1—N1	1.947(5)	Mo2—O11	2.297(4)
Co1—N2	1.935(5)	Mo2—O10	2.398(4)
Co1—N3	1.952(5)	Mo3—O3	1.697(5)
Mo1—O8	1.698(5)	Mo3—O4	1.703(5)
Mo1—O1	1.700(5)	Mo3—O7^{i}	1.903(4)
Mo1—O5	1.915(4)	Mo3—O6	1.921(4)
Mo1—O6	1.928(4)	Mo3—O12	2.356(4)
Mo1—O12	2.296(4)	Mo3—O11^{i}	2.356(4)
Mo1—O10	2.386(4)	V1—O13	1.657(5)
Mo2—O2	1.695(5)	V1—O10^{i}	1.773(4)
Mo2—O9	1.710(4)	V1—O11	1.777(4)
Mo2—O5	1.900(4)	V1—O12	1.813(4)
Mo2—O7	1.935(4)	O10^{i}—V1—O12	107.51(19)
O13—V1—O10^{i}	111.0(2)	O11—V1—O12	109.35(19)
O13—V1—O11	110.1(2)	N2—Co1—N1	84.44(19)
O10^{i}—V1—O11	108.83(19)	N2—Co1—N3	87.70(19)
O13—V1—O12	109.9(2)	N1—Co1—N3	92.63(19)

^{i}0.5−*x*, 0.5−*y*, 1−*z*.

Table 3. Selected bond distances (Å) and angles (°) for **2**.

Co1—N1	1.921(11)	Mo3—O3	1.63(1)
Co1—N1^{i}	1.921(11)	Mo3—O5	1.843(8)
V1—O13	1.618(7)	Mo3—O11	1.851(9)
V1—O12	1.686(12)	Mo3—O10	1.946(9)
Mo1—O1	1.681(9)	Mo3—O6^{iv}	1.974(8)
Mo1—O9	1.870(9)	Mo3—O13	2.368(7)
Mo1—O10	1.935(9)	Mo4—O4	1.676(9)
Mo1—O11^{iii}	1.950(8)	Mo4—O6	1.832(8)
Mo1—O8	1.958(9)	Mo4—O7	1.867(8)
Mo1—O13	2.338(7)	Mo4—O9	1.987(9)
Mo2—O2	1.680(9)	Mo4—O7^{iv}	2.014(8)
Mo2—O14	1.812(9)	Mo4—O12	2.331(6)
Mo2—O8	1.876(9)	Na2—O2W	2.352(12)
Mo2—O5	2.004(8)	Na1—O3W	2.30(3)
Mo2—O14^{iv}	2.006(10)	Na1—O1W	2.316(11)
Mo2—O13	2.369(8)	Na2—O4W	2.11(5)
N(1)–Co(1)–N(2)	83.8(4)	O(3)–Mo(3)–O(13)	170.0(4)
O(13)–V(1)–O(12)	108.3(3)	O(10)–Mo(3)–O(13)	72.8(3)
O(1)–Mo(1)–O(13)	168.2(4)	O(4)–Mo(4)–O(12)	167.6(4)
O(8)–Mo(1)–O(13)	72.6(3)	O(9)–Mo(4)–O(12)	83.7(3)
O(2)–Mo(2)–O(13)	166.7(4)	V(1)–O(12)–Mo(4)	123.2(2)
O(5)–Mo(2)–O(13)	71.5(3)	V(1)–O(13)–Mo(1)	125.4(4)

^{i}1−*y*, *x*−*y*, *z*; ^{iii}1−*y*, 2+*x*−*y*, *z*; ^{iv}−1−*x*+*y*, 1−*x*, *z*.

a powerful and effective method for synthesizing organic–inorganic hybrid materials. In a specific hydrothermal process, many factors affect the formation and crystal growth of the product phases, such as initial reactants, starting concentration, pH, reaction time, and temperature [12, 13]. Parallel experiments suggest that the starting concentration of the reaction system, the starting pH (for **1**, pH = 5.5; for **2**, pH = 4.7) and the time of reaction (for **1**, 80 h; for **2**, 144 h) are crucial for formation and crystallization of **1** and **2**. At lower pH (3.0–4.5), we cannot obtain crystals of **1** and **2**

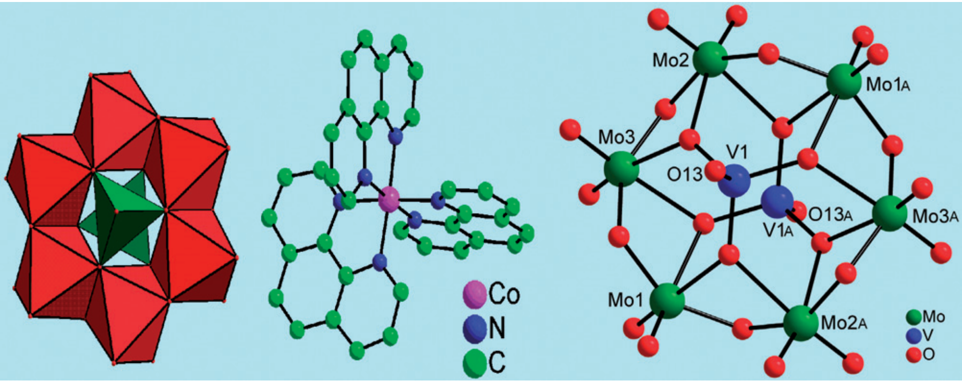

Figure 1. (Left) Polyhedral/ball-and-stick representation of the molecular structural unit of **1**. The isolated water molecules, protons, and H atoms attached to phen ligands are omitted for clarity. Color code: MoO_6, red; VO_4, pink; CoN_6, turquoise. (Right) Ball-and-stick representation of the $[V_2Mo_6(OH)_2O_{24}]^{4-}$ polyoxoanion.

suitable for single crystal X-ray diffraction. At higher pH (6.0–8.0), no crystalline phase is obtained, only powders, probably related to the difficult formation of the skeleton structure of the polyoxoanions at higher pH.

3.2. *Structural descriptions of 1 and 2*

The molecular structural unit of **1** consists of a $[V_2Mo_6(OH)_2O_{24}]^{4-}$ (according to the results of bond valence sum (BVS) calculations [14] for all oxygen atoms in the polyoxoanion, two protons should be attached to the two terminal oxygens (O13, BVS = 1.48) of VO_4 units), a $[Co(phen)_3]^{2+}$, two H^+, and seven lattice waters (figure 1 (left)). In $[V_2Mo_6(OH)_2O_{24}]^{4-}$, three types of oxygens are found: the terminal oxygen O_t (O1, O2, O3, O4, O8, O9, and O13), double-bridging oxygen $O_{\mu2}$ (O5, O6, and O7) and triple-bridging oxygen $O_{\mu3}$ (O10, O11, and O12). The Mo–O_t, Mo–$O_{\mu2}$, and Mo–$O_{\mu3}$ distances vary from 1.695(5) to 1.740(4), from 1.900(4) to 1.935(4), and from 2.296(4) to 2.398(4) Å with average lengths of 1.701, 1.917, and 2.349 Å, respectively. The V–O bond lengths can be grouped into two sets: V–O_t (1.657(5) Å) and V–$O_{\mu3}$ (1.773(4)–1.813(4) Å). These MoO_6 octahedra and VO_4 tetrahedra are severely distorted [9]. The structure of $[V_2Mo_6(OH)_2O_{24}]^{4-}$ consists of six MoO_6 and two VO_4 units, and the structure of $[V_2Mo_6(OH)_2O_{24}]^{4-}$ is very similar to that of the $\{P_2Mo_5\}$ cluster, described as two PO_4 units capping either side of a ring of five distorted MoO_6 units linked by one corner-sharing and four edge-sharing motifs [15]. However, in $[V_2Mo_6(OH)_2O_{24}]^{4-}$, it is worth noting that six MoO_6 octahedra are linked by sharing oxygens (O5, O6, and O7) forming a $\{Mo_6\}$ ring, and two VO_4 tetrahedra cap opposite sides of the $\{Mo_6\}$ ring. Each VO_4 tetrahedron is linked to three μ_3-oxygens (O10, O11, and O12) of the $\{Mo_6\}$ ring. In turn, each μ_3-oxygen links two molybdenums and a vanadium, the fourth oxygen (O13) of VO_4 is pendant (figure 1 (right)). In $[Co(phen)_3]^{2+}$ the Co(1) is a distorted CoN_6 octahedron, defined by six nitrogens from three phen with Co–N distances in the range of 1.935(5)–1.952(5) Å (average of 1.945(2) Å), comparable with those of previous study [16]. In **1**, there exist electrostatic interactions between $[V_2Mo_6(OH)_2O_{24}]^{4-}$ and $[Co(phen)_3]^{2+}$ owing to the presence of

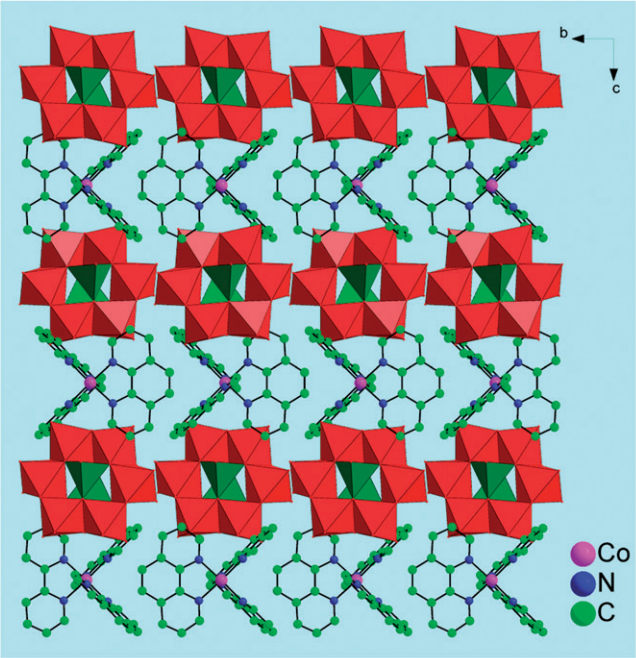

Figure 2. Packing diagram of **1** viewed down the *a*-axis. Color code: VO_4, green; MoO_6, red.

anions and cations. In addition, there also exist weak supramolecular interactions between $[V_2Mo_6(OH)_2O_{24}]^{4-}$ polyoxoanions, $[Co(phen)_3]^{2+}$ coordination cations and lattice water molecules from surface oxygens (acceptors) of $[V_2Mo_6(OH)_2O_{24}]^{4-}$ polyoxoanions, the carbon–hydrogen bonds (donors) of $[Co(phen)_3]^{2+}$ coordination cations and the oxygen-hydrogen bonds (donors) of lattice water. These electrostatic and supramolecular interactions are responsible for the stability of **1**. In the *bc* crystallographic plane, molecular structural units $[Co(phen)_3]H_2[H_2V_2Mo_6O_{26}]$ of **1** are closely aligned in –ABAB– stacking (figure 2).

Compound **2** consists of $[VMo_{12}O_{40}]^{3-}$ and $[Co(2,2'\text{-bipy})_3]^{2+}$ as well as a Na^+ countercation (figure 3). The $[VMo_{12}O_{40}]^{3-}$ is a well-known Keggin structure formed by a central VO_4 tetrahedron and 12 surrounding MoO_6 octahedra linked in corner-sharing and edge-sharing modes. The Mo–O_t, Mo–$O_{b,c}$ and Mo–O_a bond distances are 1.63(1)–1.681(9), 1.812(9)–2.014(8) and 2.331(6)–2.369(8) Å (average lengths of 1.668, 1.921 and 2.352 Å, respectively). The O–Mo–O angles fall in the range of 71.5(3)–168.2(4)°. Comparing the Mo–O_t bond lengths of $[VMo_{12}O_{40}]^{3-}$ with that of $[V_2Mo_6(OH)_2O_{24}]^{4-}$, the Mo–$O_t$ bond lengths of $[VMo_{12}O_{40}]^{3-}$ are a little shorter, in agreement with previous study [17]. For the VO_4 tetrahedron, the V–O bond lengths are in the range of 1.618(7)–1.686(12) Å (average of 1.636 Å), while the O–V–O angles vary from 108.3(3)° to 110.6(3)°. These results indicate that the MoO_6 octahedra and VO_4 tetrahedron are somewhat distorted. In $[Co(2,2'\text{-bipy})_3]^{2+}$, the Co^{2+} is octahedral defined by six nitrogens from three 2,2′-bipy with Co–N bond distances in the range 1.921(11)–1.929(10) Å (average of 1.925(2) Å). Dihedral angles among the three ideal 2,2′-bipy planes in $[Co(2,2'\text{-bipy})_3]^{2+}$ are 80.8°, 83.6° and 88.2°, not vertical to each other. The geometrical distortion of $[VMo_{12}O_{40}]^{3-}$ and $[Co(2,2'\text{-bipy})_3]^{2+}$ ions may be related to

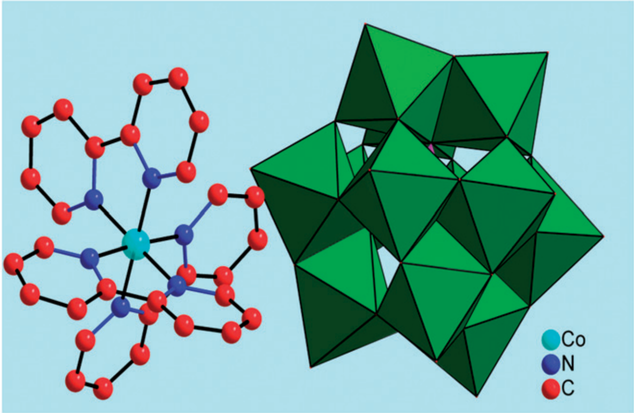

Figure 3. Polyhedral/ball-and-stick representation of the molecular structural unit of **2**. Color code: MoO_6, green; VO_4, pink. Na^+ ions and H atoms attached to 2,2′-bipy ligands are omitted for clarity.

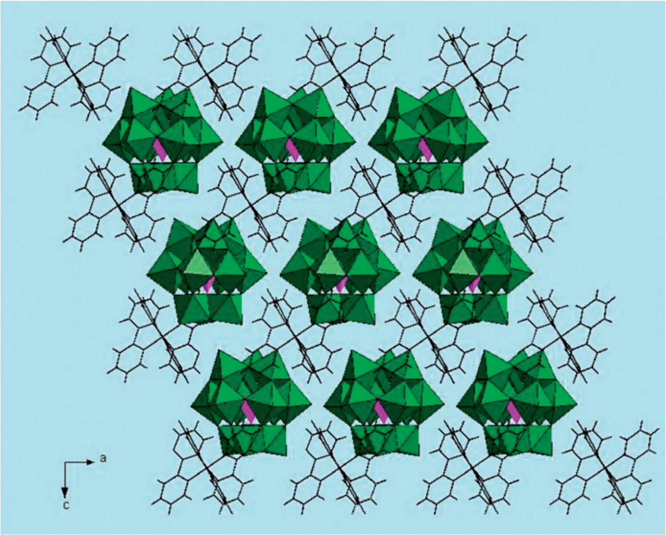

Figure 4. The crystal packing of **2** along the *b* axis. Color code: MoO_6, green; VO_4, pink.

the weak interactions between $[VMo_{12}O_{40}]^{3-}$ polyoxoanions and $[Co(2,2'\text{-bipy})_3]^{2+}$ cations, which are further supported by IR spectra. In the *ac* crystallographic plane, molecular structural units $[Co(2,2'\text{-bipy})_3][Na(H_2O)_7][VMo_{12}O_{40}]$ of **2** are closely aligned in –ABAB– stacking (figure 4). Similar to **1**, there also exist the electrostatic and supramolecular interactions between $[VMo_{12}O_{40}]^{3-}$ polyoxoanions and $[Co(2,2'\text{-bipy})_3]^{2+}$ cations.

3.3. *IR and UV spectra*

In the IR spectrum of **1**, absorption bands at 948 and 896 cm^{-1} are assigned to $\nu(M\text{–}O_t)$ ($M = Mo$ or V) stretches, and absorptions at 851, 800, 773, 698, and 636 cm^{-1}

correspond to the ν(Mo–O–M) (M = Mo or V) stretches [17–19]. A series of absorptions in the 1633–1100 cm^{-1} region indicate the presence of phen. The absorption at 3450 cm^{-1} is assigned to water. In the IR spectrum of **2**, four characteristic absorption bands at 937, 785, 762, and 896 cm^{-1} resulted from the Keggin-type polyoxoanions $[VMo_{12}O_{40}]^{3-}$, assigned to the ν(Mo–O_t), ν(Mo–O_b), ν(Mo–O_c), and ν(V–O_a) stretches, respectively. Comparing the IR spectrum of **2** with that of $(n\text{-}Bu_4N)_3VMo_{12}O_{40}$, [10], the Mo–$O_t$ absorption band shifts from 958 to 937 cm^{-1}; the Mo–O_b, Mo–O_c, and V–O_a absorptions shift from 840 to 785 cm^{-1}, from 766 to 762 cm^{-1}, and from 885 to 896 cm^{-1}, indicating that there may exist electrostatic and supramolecular interactions between $[VMo_{12}O_{40}]^{3-}$ polyoxoanions and $[Co(2,2'\text{-bipy})_3]^{2+}$ cations. In addition, a series of absorptions in the range of 1600–1100 cm^{-1} are characteristic of 2,2′-bipy. The absorption peak at 3493 cm^{-1} is assigned to water.

UV spectra of **1** and **2** are measured from 190 to 400 nm in aqueous solution (Supplementary material). The UV spectrum of **1** exhibits one band centered at 205 nm, attributed to charge-transition absorption $O_t \rightarrow Mo$ [20]. The UV spectrum of **2** in water exhibits two absorptions, a strong absorption at 208 nm and a weaker absorption at 270–300 nm. The higher energy absorption is ascribed to the charge transfer transitions $O_t \rightarrow Mo$ and the lower energy absorption to the charge transfer transitions $O_{b(c)} \rightarrow Mo$ [21].

3.4. *XPS spectra*

The BVS calculations [22] suggest that all Mos are in the +6 oxidation state and Co is in the +2 oxidation state in both **1** and **2**. The bond valence analysis also shows that V atoms are +5. The XPS spectra of **1** and **2** further confirm the calculated results. The XPS spectra of **1** in the energy regions of $Mo3d_{5/2}$, $Co2p_{3/2}$ and V2p show peaks at 232.6, 781.0, and 516.7 eV [23–27], attributable to Mo^{6+}, Co^{2+}, and V^{5+}, respectively. The XPS spectra of **2** in the energy regions of $Mo3d_{5/2}$, $Co2p_{3/2}$ and V2p show peaks at 232.6, 781.0, and 516.6 eV, attributable to Mo^{6+}, Co^{2+}, and V^{5+}, respectively. These results further confirm the valences of Mo, Co, and V.

3.5. *Thermal property*

Thermal behavior of **1** and **2** were investigated under flowing N_2 from 20°C to 700°C (Supplementary material). The TG curve for **1** exhibits two steps of weight loss. The first is 7.2% (Calcd 6.9%) in the range of 25–132°C, corresponding to the release of seven waters of crystallization. The second weight loss is 32.1% (Calcd 31.6%) from 214°C to 576°C, assigned to decomposition of three phen ligands and dehydration of four protons. The TG curve for **2** can also be divided into two stages. In the first stage, the weight loss of 5.13% (Calcd 5.01%) in the range of 32–134°C is due to loss of seven waters. In the second stage, the weight loss of 18.82% (Calcd 18.60%) in the range 216–565°C is assigned to the decomposition of three 2,2′-bipy ligands.

Supplementary material

Crystallographic data for the structural analysis reported in this article have been deposited with the Cambridge Crystallographic Data Centre with the deposited CCDC numbers 696894, 715946 for **1** and **2**. Copies of this information may be obtained free of charge from The Director, CCDC, 12 Union Road, Cambridge, CB2 1EZ, UK (Fax: +44-1223-336033; Email: deposit@ccdc.cam.ac.uk).

Acknowledgments

This work was financially supported by the National Natural Science Foundation of China, the program for New Century Excellent Talents in University of Henan Province, the Foundation of Education Department of Henan Province, and the Natural Science Foundation of Henan Province.

References

[1] E. Coronado, C.J. Gomez-Garcia. *Chem. Rev.*, **98**, 273 (1998).
[2] J.Y. Niu, Q. Wu, J.P. Wang. *J. Chem. Soc., Dalton Trans.*, **12**, 2512 (2002).
[3] C. Eugenio, R. José, G. Carlos, J. Carlos, R. Concepció, T. Judit, T. Smail, V. Jaume. *J. Mater. Chem.*, **8**, 313 (1998).
[4] B. Solsona, F. Ivars, P. Concepción, J.M.L. Nieto. *J. Catal.*, **250**, 128 (2007).
[5] L.C.W. Baker, D.C. Glick. *Chem. Rev.*, **98**, 3 (1998).
[6] S. Cevik, Z. Alkan, M. Poyraz, M. Sarı, O. Büyükgüngör. *Cryst. Res. Technol.*, **42**, 955 (2007).
[7] C.M. Liu, D.Q. Zhang, D.B. Zhu. *Cryst. Growth Des.*, **6**, 524 (2006).
[8] C.L. Pan, J.Q. Xu, Y. Sun, D.Q. Chu, L. Ye, Z.L. Lü, T.G. Wang. *Inorg. Chem. Commun.*, **6**, 233 (2003).
[9] S.W. Zhang, G.Q. Huang, Y.G. Wei, M.C. Shao, Y.Q. Tang. *Acta Cryst. C*, **49**, 1446 (1993).
[10] S.B. Jing, W.C. Zhu, J.Q. Guan, Z.L. Wang, G.J. Wang. *Acta Chim.*, **64**, 1881 (2006).
[11] N. Casañ-Pastor, C. Louis, W. Baker. *J. Am. Chem. Soc.*, **114**, 10384 (1992).
[12] K. Pavani, A. Ramanan. *Eur. J. Inorg. Chem.*, **4**, 3080 (2007).
[13] K. Pavani, S.E. Lofland, K.V. Ramanujachary, A. Ramanan. *Eur. J. Inorg. Chem.*, 568 (2005).
[14] I.D. Brown, D. Altermatt. *Acta Crystallogr. B*, **41**, 244 (1985).
[15] X.M. Lu, X.J. Wang, P.Z. Li, X.H. Pei, C.H. Ye. *J. Mol. Struct.*, **872**, 129 (2008).
[16] J.Y. Niu, Z.L. Wang, J.P. Wang. *Polyhedron*, **23**, 773 (2004).
[17] W.J. Wang, L. Xu, Y.G. Wei, F.Y. Li, G.G. Gao, E.B. Wang. *J. Solid State Chem.*, **178**, 608 (2005).
[18] A. Müller, M. Koop, P. Schiffels, H. Bögge. *Chem. Commun.*, 1715 (1997).
[19] L.M. Duan, C.L. Pan, J.Q. Xu, X.B. Cui, F.T. Xie, T.G. Wang. *Eur. J. Inorg. Chem.*, 2578 (2003).
[20] J.Y. Niu, M.L. Wei, J.P. Wang, D.B. Dang. *Eur. J. Inorg. Chem.*, 160 (2004).
[21] J.Y. Niu, M.L. Wei, J.P. Wang, D.B. Dang. *J. Mol. Struct.*, **655**, 171 (2003).
[22] N.E. Brese, M. O'Keeffe. *Acta Crystallogr. B*, **47**, 192 (1991).
[23] N.S. McIntyre, D.D. Johnston, L.L. Coatsworth, R.D. Davidson, J.R. Brown. *Surf. Interface Anal.*, **15**, 265 (1990).
[24] G.J. Zhang, Z.H. Chen, T. He, H.H. Ke, Y. Ma, K. Shao, W.S. Yang, J.N. Yao. *J. Phys. Chem. B*, **108**, 6944 (2004).
[25] C.A. Bessel, D.R. Rolison. *J. Phys. Chem. B*, **101**, 1148 (1997).
[26] J. Kasperkiewicz, J.A. Kovacich, D. Lichtman. *J. Electron Spectrosc. Relat. Phenom.*, **32**, 128 (1983).
[27] R. Larsson, B. Folkesson, G. Schön. *Chem. Scr.*, **3**, 88 (1973).